

Supplementary Information

Terahertz semiconductor laser chaos

Binbin Liu^{1,2,9}, Carlo Silvestri^{3,9}, Kang Zhou^{1,5,9}, Xuhong Ma^{1,2}, Shumin Wu^{1,2}, Ziping Li¹, Wenjian Wan¹, Zhenzhen Zhang¹, Ying Zhang⁴, Junsong Peng⁴, Heping Zeng^{4,5*}, Cheng Wang⁶, Massimo Brambilla⁷, Lorenzo Columbo^{8,*}, and Hua Li^{1,2*}

¹ State Key Laboratory of Materials for Integrated Circuits and Key Laboratory of Terahertz Solid State Technology, Shanghai Institute of Microsystem and Information Technology, Chinese Academy of Sciences, 865 Changning Road, Shanghai 200050, China.

² Center of Materials Science and Optoelectronics Engineering, University of Chinese Academy of Sciences, Beijing 100049, China.

³ Institute of Photonics and Optical Science (IPOS), School of Physics, The University of Sydney, NSW 2006, Australia.

⁴ State Key Laboratory of Precision Spectroscopy, East China Normal University, Shanghai 200241, China.

⁵ Chongqing Key Laboratory of Precision Optics, Chongqing Institute of East China Normal University, Chongqing 401120, China.

⁶ School of Information Science and Technology, ShanghaiTech University, 393 Middle Huaxia Road, Shanghai 201210, China.

⁷ Dipartimento Interateneo di Fisica, Politecnico di Bari and CNR-IFN (UOS Bari), Via Amendola 173, IT-70126, Italy

⁸ Dipartimento di Elettronica e Telecomunicazioni, Politecnico di Torino, Corso Duca degli Abruzzi 24, Torino, IT-10129, Italy.

⁹ These authors contributed equally.

*Corresponding authors.

E-mail: hpzeng@phy.ecnu.edu.cn; lorenzo.columbo@polito.it; hua.li@mail.sim.ac.cn

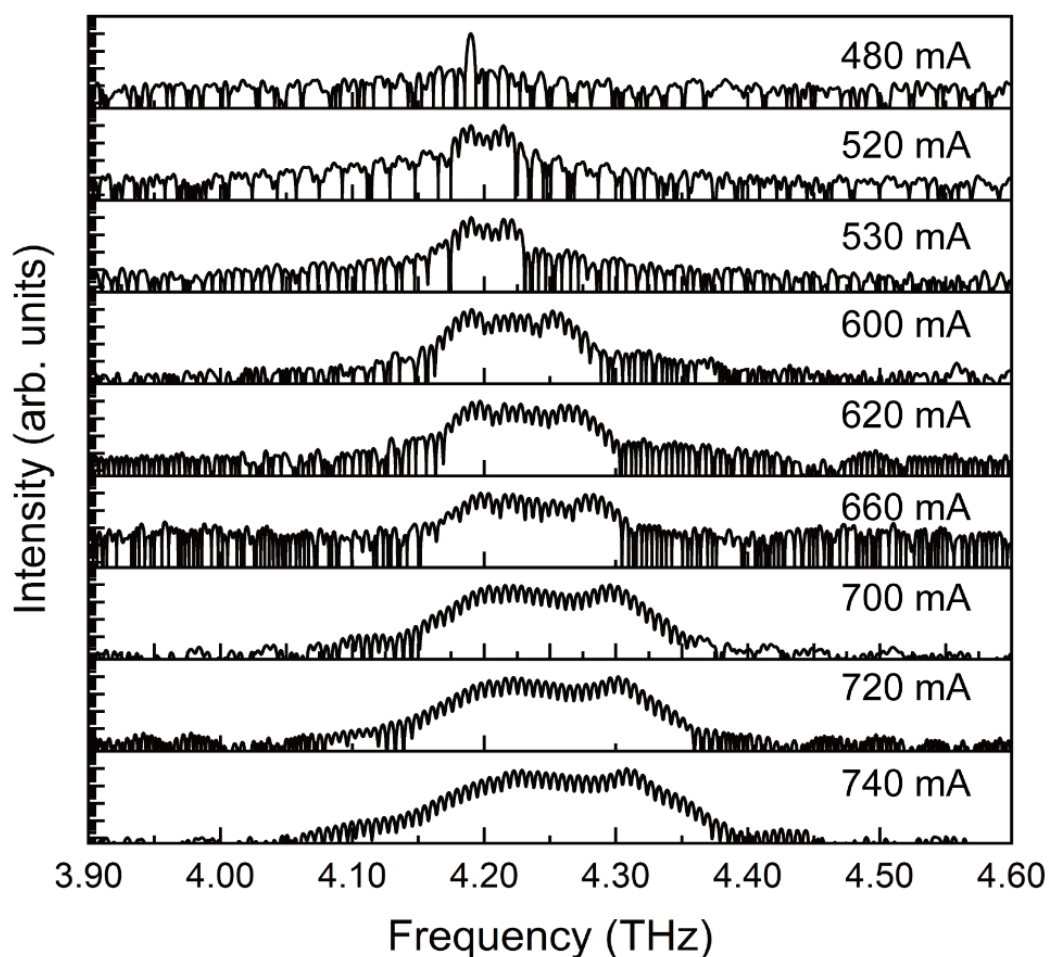


Fig. S1. Terahertz emission spectra at various currents measured using a Fourier-transform infrared (FTIR) spectrometer (Bruker, v80) with a spectral resolution of 3 GHz. To reduce the water absorption loss as much as possible, the FTIR chamber is pumped down to 3 mbar and the optical beam path outside the FTIR is purged with dry air. The terahertz light is coupled into the FTIR chamber using a parabolic mirror.

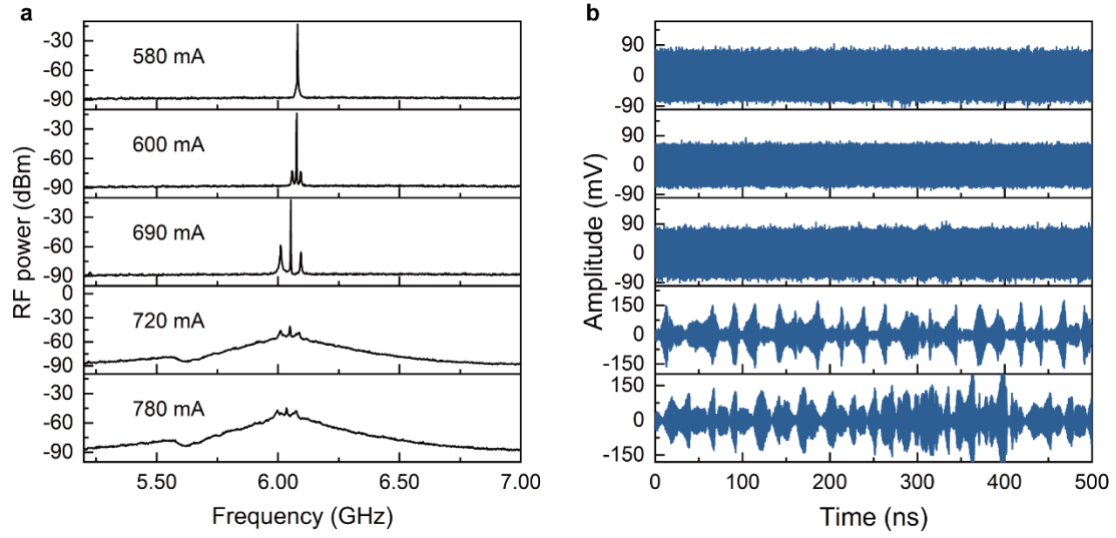


Fig. S2. (a), Electrical spectra at different currents, measured with a RBW of 10 kHz and a VBW of 1 kHz. (b), Evolution of corresponding time traces. As the current is increased from 580 to 780 mA, inter-mode BN spectra show clear transitions from single narrow peak, multi-peak and broad peak. At 580 mA, the time trace exhibits a sinusoidal period time series. As the current is increased to 600 and 690 mA, a modulation on the sinusoidal time trace is not clearly observed. The reason is that the signal-to-noise ratio of the sidebands is too low. When we further increase the current to 720 or 780 mA, typical chaotic time traces without any accurate and predictable periodicity are observed showing the laser enters the chaotic regime.

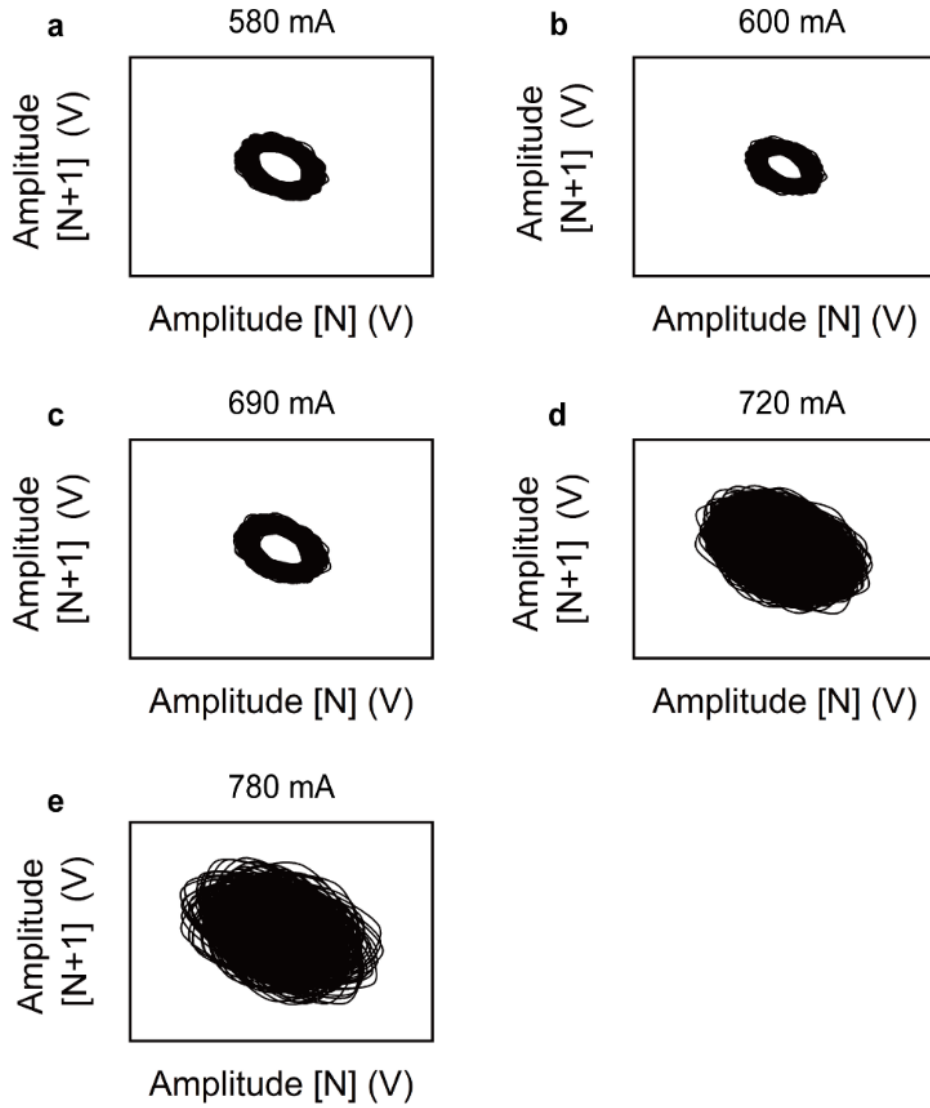


Fig. S3. Phase portraits at various currents with times series of 500 ns. A periodic system normally shows an inner circle in its two-dimensional phase portrait at 580, 600 and 690 mA. The phase portraits become more complex at 720 and 780 mA, and much stronger oscillations result in larger trajectories in phase portraits.

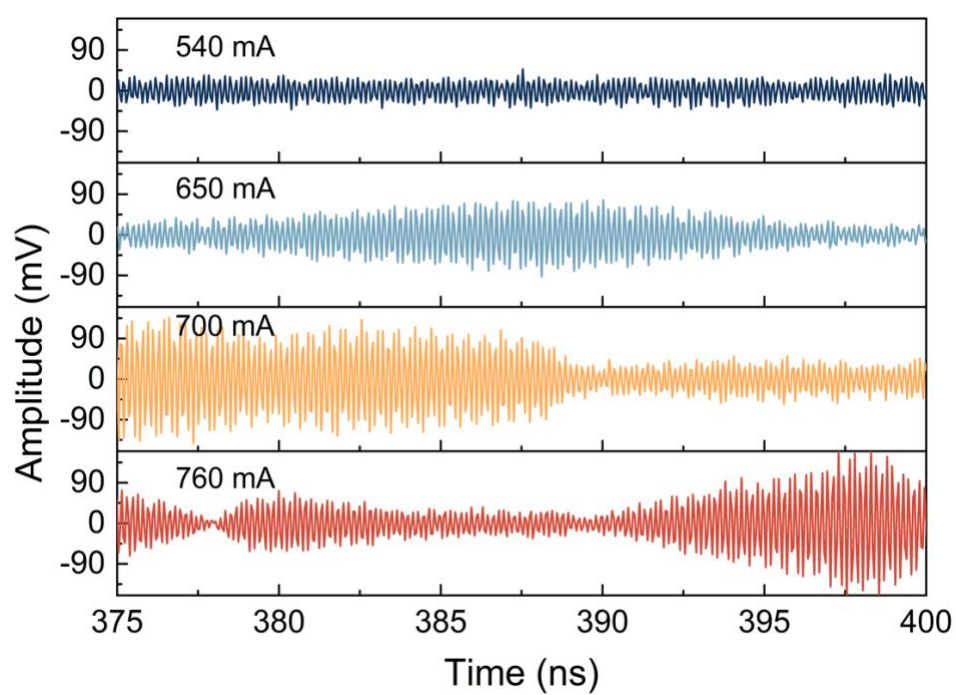


Fig. S4. Evolution of experimental time traces with a length of 25 ns at various currents.

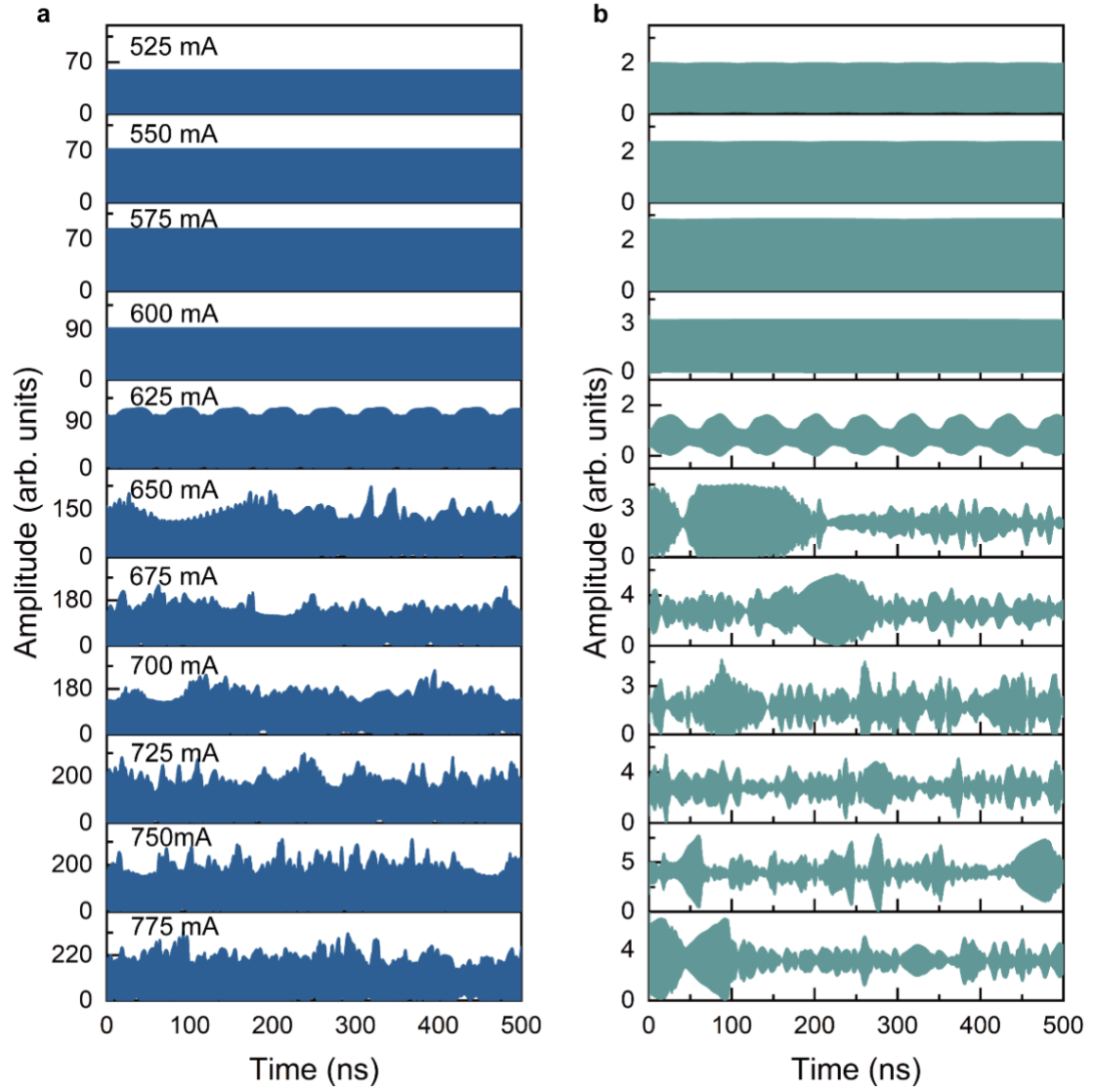


Fig. S5. Simulated results. Due to the high sampling rate in numerical calculation, the minimum time interval is 0.002 ns. To avoid the influence of higher harmonics on calculated results, we use a digital filtering method to obtain pure BN signal. (a), Time series without filtering and (b), after filtering at various currents.

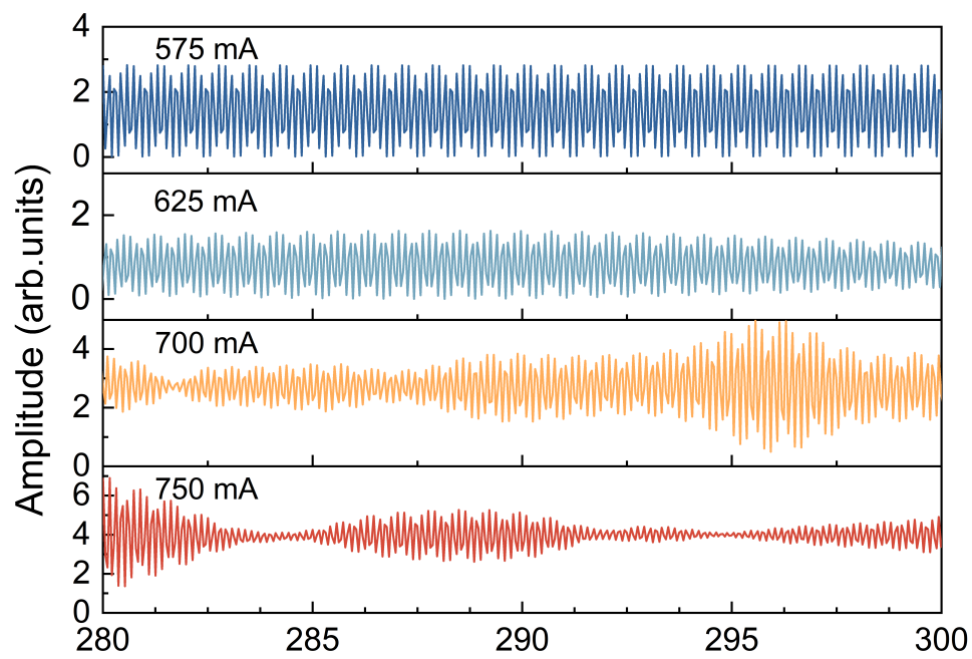


Fig. S6. Simulated time series with a length of 20 ns after filtering at various currents.

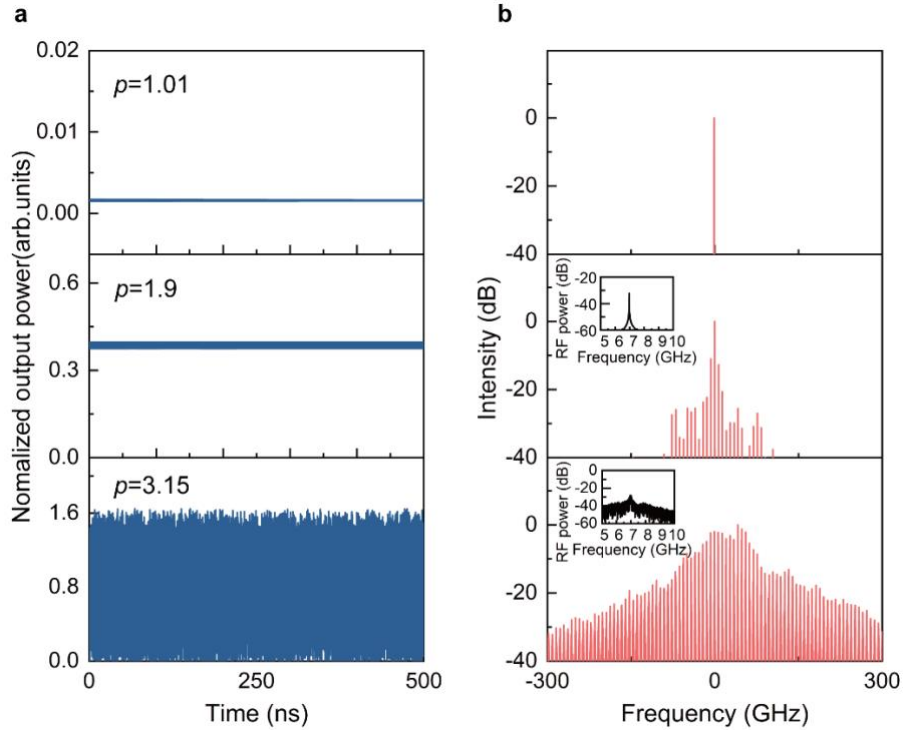


Fig. S7. Role of current p parameter to QCL's behaviors at $\alpha=1.15$ and $k''=0$. (a), Time series at $p=1.01, 1.9, 3.15$. (b), Corresponding optical spectra. The insets in b are inter-mode BN spectra. The simulated results highlight the current parameter as a critical determinant of QCL stability. When the p parameter is set to 1.01, a single-mode emission spectrum and stable time series are observed. When the p parameter is set to 1.9, the optical frequency combs emission is observed. And the QCL enters chaotic regimes when the p parameter is set to 3.15.

Table S1 Parameters used in the full model

Parameter	Quantity
Cavity length	6 mm
Background refractive index of the active medium	3.6
Waveguide losses	3.5 cm^{-1}
Volume of the active medium	$100\mu\text{m} \times 6\text{mm} \times 10\mu\text{m}$
Reflectivity of the QCL facets	0.32
Number of stages of the cascading scheme	76
Central emission frequency	4.2 THz
δ_{hom}	500 GHz
Carrier lifetime	50 ps
α factor	0.1
Confinement factor of the field in the active medium	0.25
Threshold current	390 mA
f_0	$4.5 \times 10^{-6} \mu\text{m}^3$

Table S2 Parameters used in the reduced model

Parameter	Quantity
Cavity length	6 mm
Background refractive index of the active medium	3.6
Waveguide losses	3.5 cm^{-1}
Reflectivity of the QCL facets	0.32
δ_{hom}	500 GHz
α factor	various